CONSTRAINTS ON DEPTH AND THICKNESS OF AN OBLATE MAGMA CHAMBER AT SAPAS MONS, VENUS. S. T. O'Hara[1], P. J. McGovern[1], D. W. vonLembke[1,2], [1]Lunar and Planetary Institute (USRA), Houston, TX 77058, [2]Colorado School of Mines, Golden, CO 80401.

Introduction: The Sapas Mons volcano on Venus has an edifice radius of ~150 km and flow units extending more than 300 km from the summit [1, 2]. The summit is circumscribed by a series of extensional faults (graben) and fractures. These features (Fig. 1) occur at an average radius of 50 km from the summit and may delineate the outer boundary of a subsurface magma chamber. [1]

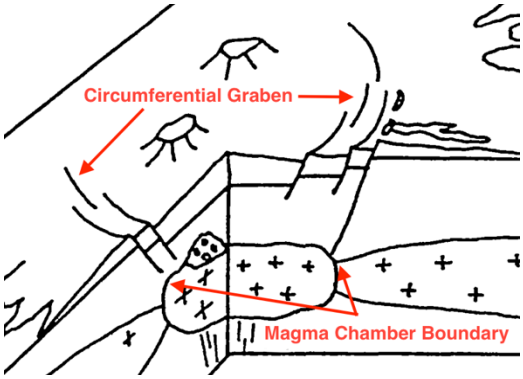

Figure 1: Detail of schematic block diagram of Sapas Mons, after Keddie and Head [1]. Arrows note relationship between failure at magma chamber margin and formation of extensional ring faults.

Gravitational loading and flexure for a volcanic edifice tends to produce compressional stresses near the summit, contrary to the extensional nature of these observed faults (Fig. 1). Previous work by this team [3] has demonstrated that a stress state consistent with graben formation can be generated by modeling the deformation of the volcanic edifice in a half-space domain, in which vertical deflections from loading and horizontal compressive stresses in the edifice remain small. This may correspond to a configuration in which the volcano is supported by dynamic forces in the mantle related to plume upwellings.

To determine the plausible extent of conditions which could generate the observed graben, we extend the previous work to investigate how magma chamber size and shape parameters affect the generation of extensional faulting.

Methods: To investigate the effect of changes in magma chamber parameters on the stress state within the edifice, we implement models of the edifice in COMSOL Multiphysics using an edifice-loaded elastic substrate in an axisymmetric geometry [e.g., 4-7]. The initial (pre-deformation) edifice has a radius of 200 km and a height of 5 km, plus an elliptical magma chamber with a radius of 50 km and of varying height and depth embedded within the substrate.

We apply a negative change in pressure normal to the boundary of this chamber to simulate withdrawal of magma due to eruptive activity, which we term "underpressure" [see 3]. We parameterize this underpressure based on a ratio of the applied pressure on the chamber boundary to the lithostatic stress at the top of the chamber. This allows us to systematically vary the underpressure independent of the changes in overlying load due to chamber size and position. In addition, we explicitly incorporate the effects of the atmospheric pressure of Venus into our model, which was not included in [3].

The models calculate horizontal normal stresses in the plane of the model (σ_r, the "radial" stress) and perpendicular to the plane (σ_θ, the "hoop" stress) as well as the vertical normal stress σ_z. We use a tension-positive sign convention. We calculate differential stress σ_D as the difference between the greatest and least principal normal stresses. We also calculate the "proximity to failure" (P_F) parameter, a measure of how close a given stress state is to failure according to the Mohr-Coulomb failure criterion. A P_F value of 1 indicates that faulting is predicted at that location [8].

Results and Discussion: Chamber height varies between 500 m and 2 km, while the depth varies between 1 km and 7 km. Parameter combinations that result in chambers that extend into the edifice are discarded. For each model run, the underpressure ratio applied to the chamber boundary is adjusted until P_F exceeds 1 at the surface near the radius of the chamber margin (50 km). This represents the minimum underpressure required for extensional failure to occur. Underpressure is then continually adjusted upwards until P_F exceeds 1 at the summit, which represents the start of compressional failure. This value is the maximum underpressure possible for *only* extensional failure at this set of chamber parameters.

Byrne et al. [9] have suggested that cryptic compressional faulting ("terracing") may be pervasive near the summits of planetary volcanoes. Due to the low resolution of the Magellan images of Sapas Mons, we cannot rule out that some cryptic compressional faulting has occurred. Therefore, we extend our parameter sweep to allow P_F to exceed 1 within a 10 km radius of the summit as well.

In general we find that the magnitude of underpressure required to reach failure increases with the depth of the chamber, as noted in [3]. Conversely, underpressure required for failure decreases with the relative height of the chamber; on average a chamber 1.5 km in height requires 15% less underpressure to achieve failure than one with a height of 500 m at the same depth.

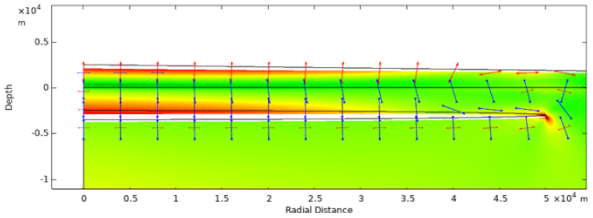

Figure 2: Differential stress plot of a gravitationally loaded edifice above an elliptical magma chamber. Colors indicate magnitude of stress; arrows indicate principal stress direction (red extensional, blue compressional.)

The reason for this relationship becomes apparent when viewing a plot of the differential stress underneath the edifice (Figure 2). The extremely oblate magma chamber has essentially bifurcated the portion of the plate overlying the magma chamber into a separate quasi-plate structure, which is undergoing a classical flexural response as it deflects downward into the chamber. The chamber in turn exerts a restoring force based on the chamber wall pressure. Thinning of this "plate," with a combination of either shallow or lower aspect ratio chambers, increases the flexural response, while deeper and higher aspect ratio chambers attenuate it.

Magma chambers deeper than approximately 5.5 km are too deep to effectively interact with the surface before underpressure values become high enough for the chamber to collapse prior to extensional margin failure.

This leaves a confined parameter space in which extensional margin failure can occur without compressional summit failure. This parameter space is expanded slightly if we allow for near-summit cryptic compressional failure as per [9] (Figure 3). Conditions most favorable to the observed faulting generally occur at depths between 2 to 4 km, and strongly favor narrow, high aspect ratio chambers.

Conclusions and Future Directions: We find that the extensional ring faults observed on Sapas Mons can be adequately explained by margin failure of a deflating, oblate magma chamber. Failure is most favored in situations where the magma chamber has a high aspect ratio and is at a depth of 2 to 4 km beneath the edifice. The narrowness of the chamber is consistent with findings that other Venus volcanoes likely possess oblate, sill-like magma chambers [11, 12], suggesting that this geometry may be pervasive on Venus. Limited compressional faulting at the summit as a result of flexure of the edifice into the underlying chamber may also occur if it is limited to a scale below the resolution of Magellan imagery.

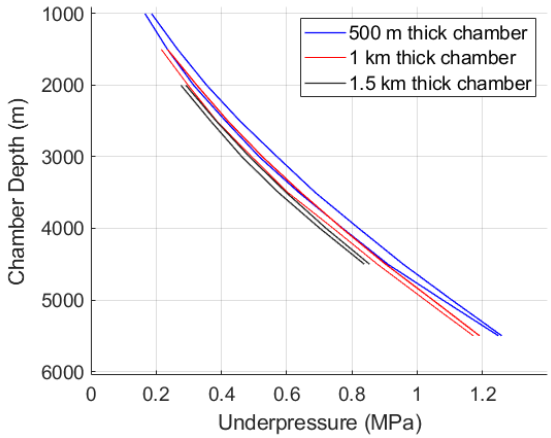

Figure 3: Chamber depth vs. underpressure for chambers of varying height. Area between two curves indicates parameter space where extensional margin failure plus limited summit compressional failure can occur.

Acknowledgments: This material is based upon work supported by NASA through the Lunar and Planetary Institute (LPI) and also by NASA Grant 80NSSC18K0009 (SSW). The LPI is operated by Universities Space Research Association (USRA) under a cooperative agreement with the Science Mission Directorate of NASA.

References: [1] S.T. Keddie and J.W. Head (1994) Earth, Moon, and Planets, 65.2, 129-190. [2] P.J. McGovern and S.C. Solomon (1997) *J. Geophys. Res. Planets*, *102.E7*, 16303-16318. [3] D.W. vonLembke et al. (2022) *LPSC 53*, Abstract #1761 [4] E. Grosfils (2007) *J. Volcan. And Geotherm. Res.*, *166.2*, 47-75; [5] G.A. Galgana et al. (2011) *J. Geophys. Res. Planets, 166.E3* [6] N. Le Corvec et al. (2015) *J. Geophys. Res. Planets 120.7,* 1279-1297. [7] G.A. Galgana et al. (2013) *Icarus, 255, 538-547*. [8] P.J. McGovern and S.C. Solomon (1993) *J. Geophys. Res. Planets 98.E12,* 23553-23579. [9] P.K. Byrne et al. (2009) *Earth and Plan. Sci. Let. 281.1-2*, 1-13. [10] McGovern and Solomon (1998) *J. Geophys Res., 103*, 11,071-11,101. [11] McGovern et al. (2001), *J. Geophys. Res., 106*, 23,769-23,809. [12] P.J. McGovern et al. (2014) *Geology, 42.1*, 59-62.